

Mode separation of the Josephson plasma in $\text{Bi}_2\text{Sr}_2\text{CaCu}_2\text{O}_{8+\delta}$

Itsuhiro Kakeya and Koichi Kindo

Research Center for Materials Science at Extreme Conditions (KYOKUGEN), Osaka University, Toyonaka, Osaka 560, Japan

Kazuo Kadowaki

Institute of Materials Science, The University of Tsukuba, Tsukuba, Ibaraki 305, Japan

Saburo Takahashi

Institute for Materials Research, Tohoku University, Sendai 980-77, Japan

Takashi Mochiku

National Institute for Metals, Tsukuba, Ibaraki 305, Japan

(Received 7 July 1997)

The Josephson plasma resonance in single-crystalline $\text{Bi}_2\text{Sr}_2\text{CaCu}_2\text{O}_{8+\delta}$ has been investigated at a microwave frequency of 35 GHz in a TE_{102} cavity resonator as functions of external magnetic field ($\mathbf{H}_{\text{ext}} \parallel c$ axis), temperature, and sample dimension L of the ab plane. A sharp resonance is observed in a perpendicular oscillating electric field ($\mathbf{E}_{\text{rf}} \parallel c$), whereas multi-peaks are found in a parallel oscillating magnetic field ($\mathbf{H}_{\text{rf}} \parallel ab$). The former is independent of the sample dimension, while the latter shifts to higher fields as the sample size L is reduced, and it disappears when L becomes smaller than the critical length L^* . At 35 GHz, the value of L^* is obtained to be 1.6 mm. The size-dependent resonance observed in $\mathbf{H}_{\text{rf}} \parallel ab$ can be explained by the strong dispersion relation of the transverse Josephson plasma, while the size independence of the resonance in $\mathbf{E}_{\text{rf}} \parallel c$ can be described by the longitudinal Josephson plasma as predicted by the recent theory of Josephson plasma of Tachiki *et al.* Since the longitudinal plasma mode is the Nambu-Goldstone mode in a superconductor, the experimental distinction between the longitudinal and the transverse mode leads to the conclusion that the existence of the Nambu-Goldstone mode as predicted by Anderson was experimentally confirmed by direct observation of the Josephson plasma resonance with longitudinal excitations. The finite gap found in the Josephson plasma resonance also provides a direct proof of the Anderson-Higgs mechanism within the context of the spontaneously broken phase symmetry of the gauge-field theory in a superconductor. [S0163-1829(98)03605-4]

I. INTRODUCTION

Since the observation of a sharp plasma edge at a far-infrared frequency region in polycrystalline high- T_c samples by Noh *et al.*,¹ and in single-crystalline $\text{La}_{2-x}\text{Sr}_x\text{CuO}_4$ by Tamasaku *et al.*,² the collective plasma mode excited by electromagnetic waves in high- T_c superconductors has attracted much attention. Tachiki *et al.*³ pointed out that this excitation is characteristic of layered superconductors coupled with the Josephson effect, and cannot be observed in conventional three-dimensional superconducting systems where the plasma excitation energy $\omega_p \sim eV$ lies well above the superconducting gap Δ of a few meV.⁴ In high- T_c superconductors such as $\text{Bi}_2\text{Sr}_2\text{CaCu}_2\text{O}_{8+\delta}$, it has been inferred that the well-separated layered structure may give rise to the weakly coupled superconductor-insulator-superconductor (SIS) Josephson interaction, since anomalous Josephson-junction-like behavior in I - V characteristics has been observed.⁵⁻⁸ In fact, Fertig and Das Sarma,⁹ and Mishonov¹⁰ have predicted the existence of the low-energy excitations even in the superconducting energy gap Δ in such layered systems. For example, the plasma frequency perpendicular to the layers in $\text{Bi}_2\text{Sr}_2\text{CaCu}_2\text{O}_{8+\delta}$, can be estimated to be $\omega_p = c/\sqrt{\epsilon}\lambda_c \approx 1$ meV, which is much lower than the superconducting energy gap $\Delta \approx 30$ meV.^{11,12} In such a condition, the

plasma oscillation can be expected to be observable by electromagnetic excitations since the Landau damping mechanism does not work.

The electromagnetic resonance due to the plasma oscillation in a microwave frequency region was discovered by Tsui *et al.*¹³ in the surface impedance measurement of the ab plane of $\text{Bi}_2\text{Sr}_2\text{CaCu}_2\text{O}_{8+\delta}$ in a perpendicular external field ($\mathbf{H}_{\text{ext}} \parallel c$). Subsequently, Matsuda *et al.*¹⁴ observed a sharp resonance by the experiments in a perpendicular oscillating electric field ($\mathbf{E}_{\text{rf}} \parallel c$) with a cavity resonator. They interpreted that this resonance is due to the Josephson plasma resonance as suggested by Bulaevskii *et al.*¹⁵ In those studies, it is also shown that the absorption line intensity, the width, and the position behave in a complicated fashion as functions of the external field \mathbf{H}_{ext} , the microwave frequency ν , and the temperature T , suggesting the existence of a strong coupling between the plasma modes and the vortex state. Since then, several theoretical¹⁶⁻¹⁸ and experimental¹⁹ works on the Josephson plasma phenomena in $\text{Bi}_2\text{Sr}_2\text{CaCu}_2\text{O}_{8+\delta}$ have been reported. Similar absorption phenomena have also been observed in $\text{Bi}_2(\text{Sr},\text{La})_2\text{CaCu}_2\text{O}_y$,²⁰ and in an organic superconductor κ -(BEDT-TTF)₂Cu(NCS)₂.²¹ These materials are also well known as layered superconductors which have arrays of SIS Josephson junctions similar to $\text{Bi}_2\text{Sr}_2\text{CaCu}_2\text{O}_{8+\delta}$.

A fundamental question has arisen from the recent theoretical studies. Since there exist two plasma modes, longitudinal and transverse, as collective excitations, the question is which mode has been observed experimentally. According to theory, the two modes have very different dispersion relations: the longitudinal plasma mode ($\mathbf{k}\parallel c$) has a characteristic flat dispersion, whereas the transverse one ($\mathbf{k}\perp c$) shows a strong dispersion which tends to a linear dependence for $k\rightarrow\infty$.²² As a result, the line shapes of the resonances are expected to differ considerably: for the longitudinal mode, it should be sharp and almost symmetric, while the resonance of the transverse mode has a broad and asymmetric line shape because of the long tail on the higher field side of the resonance. In order to examine the character of the two modes, experiments have been performed with various configurations of sample position and microwave fields, \mathbf{E}_{rf} and \mathbf{H}_{rf} . From these experiments, it is concluded that the resonance observed in the case of $\mathbf{E}_{\text{rf}}\parallel c$ is not the transverse plasma mode but the longitudinal one.²³ This conclusion contradicts earlier ones,^{14,15} which identified it as the transverse mode.

In this paper, we discuss in detail how to distinguish the two modes experimentally by using two configurations of plasma excitations among several possible configurations of microwave \mathbf{E}_{rf} and \mathbf{H}_{rf} vectors and the crystallographic axes of the sample: one is the case $\mathbf{E}_{\text{rf}}\parallel c$ and the other is the case $\mathbf{H}_{\text{rf}}\parallel ab$. Two plasma modes can be generated separately and independently by these two experimental conditions. The distinction of the two modes is done by making use of the sample size dependence of the plasma resonance: for the transverse mode excited in the configuration of $\mathbf{H}_{\text{rf}}\parallel ab$, a systematic shift of the resonance field was observed as a function of the sample size L in the ab plane, while for the longitudinal mode, it is independent of L according to the theoretical prediction.^{24,25} This sharp difference of the sample size effect is expected from the characteristic dispersion relation of the transverse mode.

This clear experimental evidence for two distinct plasma modes leads to an interesting corollary concerning a fundamental aspect of the superconducting transition. As is well known in the theory of phase transitions with the spontaneous symmetry breaking, the phase symmetry of the gauge field is spontaneously broken with the appearance of the superconducting phase. The collective excitations associated with the broken phase symmetry in a superconductor are known to be the longitudinal plasma mode, which is the Nambu-Goldstone mode.²⁶⁻²⁹ Therefore, the distinction of the two plasma modes made in the present experiments gives direct experimental confirmation of the existence of the Nambu-Goldstone mode in a superconductor.^{30,31} The plasma mode in a charged system such as conventional superconductors has an energy gap of the order of eV. Thus, as pointed out by Anderson, the Nambu-Goldstone mode has never been observed experimentally in the past. Furthermore, the observed energy gap of the plasma mode proves directly the validity of the Anderson-Higgs-Kibble³²⁻³⁴ mechanism for superconducting phase transition.

II. EXPERIMENT

All experiments were performed at 35 GHz. A rectangular cavity resonator with TE_{102} mode was used. It is advanta-

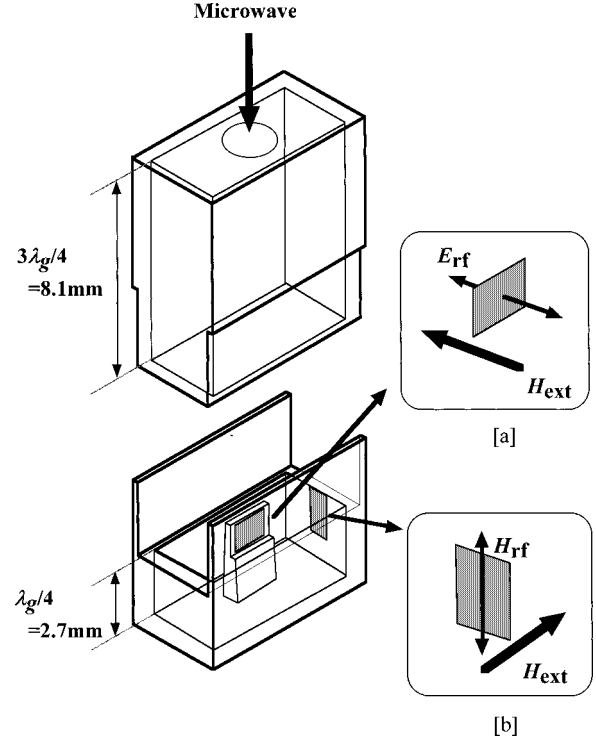


FIG. 1. Schematic view of the cavity resonator and the position of the single-crystalline $\text{Bi}_2\text{Sr}_2\text{CaCu}_2\text{O}_{8+\delta}$ sample. The cavity is made of copper waveguide of WRI-320 (JIS; WR-28 in EIA), whose inner cross section is a rectangle of $7.11\text{ mm} \times 3.56\text{ mm}$. The resonance frequency of the cavity is 35.11 GHz without load. The samples are placed at two positions corresponding to two different configurations between the microwave \mathbf{E} and \mathbf{H} vectors and crystallographic axis of the sample. Insets [a] and [b] show the geometrical relation between the sample and microwave \mathbf{E} and \mathbf{H} vectors used for longitudinal plasma and transverse plasma excitations, respectively.

geous to use the cavity resonator in order to determine the experimental configurations between oscillating electromagnetic fields, \mathbf{E}_{rf} and \mathbf{H}_{rf} , and the crystal axis of the sample. The cavity is made of a piece of copper waveguide and can be opened easily by mechanically sliding the quarter of the bottom part of the cavity as shown in Fig. 1. The measurements were performed for two samples. Superconducting transition temperatures are 90 K and 84 K for sample A and B , respectively. This was checked after all measurements were done by magnetic-susceptibility measurements in a superconducting quantum interference device magnetometer. Both samples are rectangular thick films with thickness of $20\ \mu\text{m}$. Sample A was carefully cut in several steps using a sharp knife from the initial size of $2.8\text{ mm} \times 2.5\text{ mm}$ to final size of $0.73\text{ mm} \times 0.72\text{ mm}$. At each step, resonance experiments with varying temperature were carried out for different configurations of the sample (both $\mathbf{E}_{\text{rf}}\parallel c$ and $\mathbf{H}_{\text{rf}}\parallel ab$). The sample was placed at two positions in order to have the two different configurations shown in Fig. 1. In the first case, the sample is placed at the position where \mathbf{E}_{rf} is maximum and \mathbf{E}_{rf} and \mathbf{H}_{ext} are parallel to the c axis on the sample stage made of Teflon (as shown in the inset [a]). This configuration is same as in previous experiments.^{14,23} In the second case, the samples are glued on the H plane of the cavity with grease so that \mathbf{H}_{rf} and \mathbf{H}_{ext} are parallel and perpendicular to

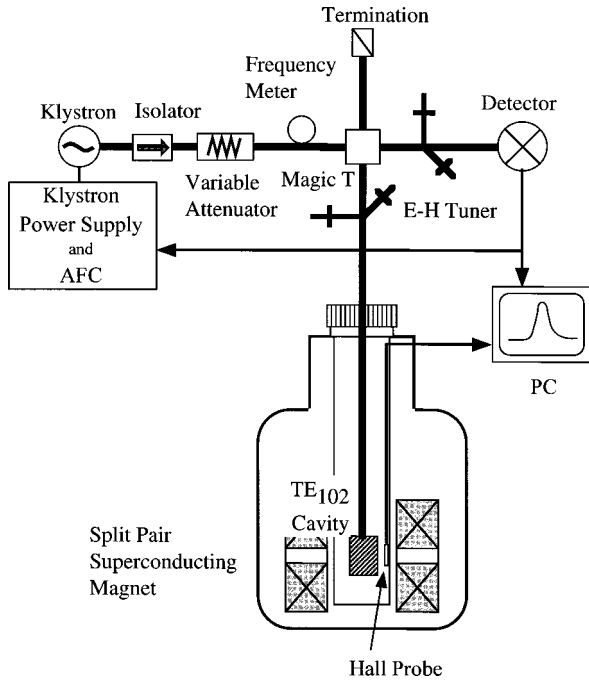


FIG. 2. Block diagram of the measuring system used in the present microwave experiment. This configuration is commonly used as an ESR spectrometer. The incident microwave frequency is stabilized by the AFC (automatic frequency controller) and the absorption is detected by a Schottky barrier diode. The superconducting magnet can generate a horizontal magnetic field up to 60 kOe.

the ab plane, respectively (as shown in the inset[b]).

We employ as the measurement system a conventional reflection-type microwave bridge which consists of a klystron, a magic tee, E-H tuners, an isolator, an attenuator, and the other components. The incident microwave power is roughly estimated to be between 50 and 10 mW, although the absorbed power was not calibrated. The absorption signal is detected as a change of cavity impedance by a semiconductor detector. In principle, this system has the advantage, in comparison with the bolometric techniques which have been previously employed, that additional phase information can be extracted from the resonance data. The block diagram of the measuring system is shown in Fig. 2.

III. EXPERIMENTAL RESULTS

A. Resonance absorption

in a perpendicular oscillating electric field ($E_{\text{rf}} \parallel c$)

For both samples, a sharp plasma resonance is observed. As an example, typical resonance lines of sample A are shown in Fig. 3, where the absorption is shown as a function of H_{ext} , applied parallel to the c axis, for various temperatures below T_c . The resonance line begins to appear just below T_c near zero field and the resonance field shifts to higher field as temperature is decreased. The resonance field shows a maximum around 25 K and decreases again as temperature is decreased. At temperatures lower than 25 K, the resonance line tends to show considerable hysteresis with field increase and decrease. It is noted that the hysteretic resonance line below 25 K shows relaxation behavior, indicating that the nonequilibrium magnetic properties are in-

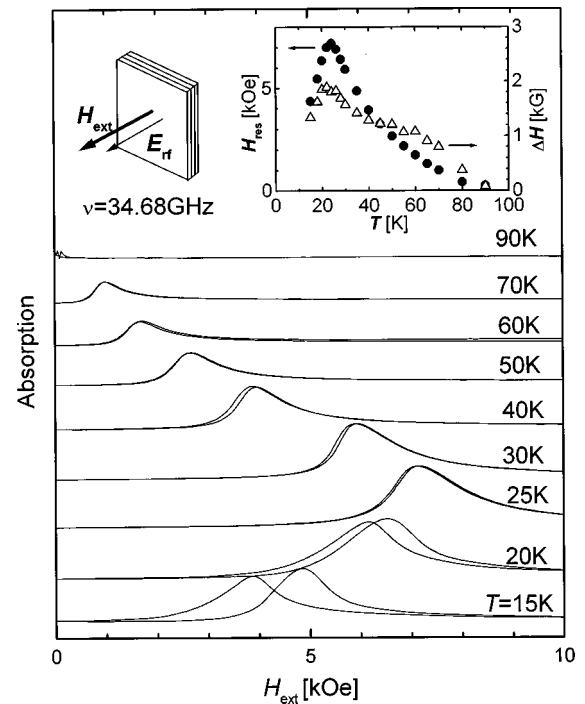


FIG. 3. Temperature dependence of the resonance line of Sample A in the configuration of $E_{\text{rf}} \parallel H_{\text{ext}} \parallel c$. The incident microwave frequency is 34.68 GHz. The shape of the resonance line is almost symmetric and has a only slight tail at a higher field side, which is the characteristic feature of the longitudinal plasma mode. The resonance field is maximum around 25 K and decreases as temperature increases approximately in proportion to $1/T$. The inset shows the plotted results of the resonance field (solid circles) and the linewidth (open triangles) as a function of temperature.

involved in this phenomenon. This hysteretic behavior is clearly seen in the data at 15 and 20 K in Fig. 3.

Another feature seen in Fig. 3 is that the resonance line shape is almost symmetric with a slight tail on the higher field side. This behavior contrasts with that for the case of $H_{\text{rf}} \parallel ab$ as described below. All these behaviors are very similar to the previous results obtained in the same condition.^{14,23} When the sample dimension in the ab plane is reduced, the position of resonance line does not move in this configuration ($E_{\text{rf}} \parallel c$). This experiment was carried out on sample B whose dimension in the ab plane was varied from 1.8 to 0.79 mm, although the lines are not shown here.

B. Resonance absorption

in a parallel oscillating magnetic field ($H_{\text{rf}} \parallel ab$)

Resonance absorption at various temperatures below $T_c = 90$ K is shown in Fig. 4 at 35 GHz with $H_{\text{rf}} \parallel ab$ (see the inset of Fig. 4). The spikelike lines at 12.48 kOe are due to the ESR signal of DPPH (1,1-dyphenil-2-picryl hydrazyl) as a field marker. The sample was a rectangular shape, 1.46 mm \times 2.40 mm \times 28 μ m, in this particular case. In this case, two distinct peaks with different characters were observed: the resonance at the lower field is sharper and relatively weaker, while the one at a higher field is broader and stronger in absorption intensity. These characteristic features of the two lines for $H_{\text{rf}} \parallel ab$ are in sharp contrast with the case for $E_{\text{rf}} \parallel c$, where only a single line is observed regardless of the sample

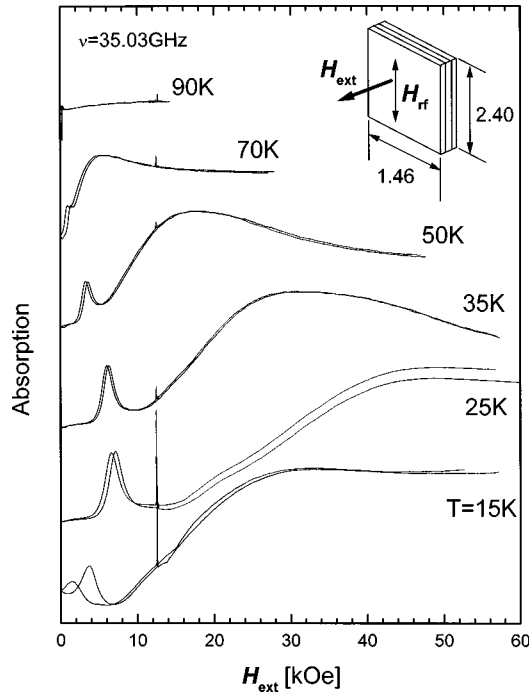


FIG. 4. The resonance absorption of sample A for a fixed dimension of the ab plane at 35.0 GHz. The oscillating magnetic field (H_{rf}) is applied parallel to the ab plane. In this particular sample dimension, two transverse Josephson plasma resonance peaks can be observed. A sharp and rather symmetric resonance is observed at lower field, whereas a broad and asymmetric resonance is seen at a higher field. A small and sharp spike at 12.48 kOe is due to the ESR signal of DPPH as a magnetic-field reference marker. The inset shows the sample geometry with configuration of the microwave H vector and the external field.

dimension L . The number of lines are determined as a function of the sample dimension for $H_{rf} \parallel ab$. In the case of larger sample dimension L , we observed multiabsorption lines (more than two). We have chosen the sample to be as large as possible for this experiment but it is restricted by the dimension of the cavity and the field homogeneity inside the cavity as seen in Fig. 1.

When the temperature is varied from 4.2 K, both resonance lines shift toward higher fields up to about 25 K, then turn to decrease to lower fields drastically. Below 25 K, the resonance curve shows the hysteretic behavior as seen in Fig. 3. It seems experimentally that such a temperature dependence of the resonance lines is common for both cases in $H_{rf} \parallel ab$ and in $E_{rf} \parallel c$. This behavior, in particular, for the case of $H_{rf} \parallel ab$ is plotted in Fig. 5, where the sharp maximum of the resonance field as a function of temperature can be seen. These maximum positions reproduce very well the irreversibility line as pointed out previously.¹³ In this figure, the temperature dependence of the resonance lines for two other sample dimensions are also added.

The observed absorption lines at 25 K at various sample sizes are displayed in Fig. 6. Here, L_{\perp} , as shown in the inset of Fig. 6, is the sample length along the direction perpendicular to H_{rf} , which is varied, and the length along the parallel direction L_{\parallel} to H_{rf} is kept constant for all L_{\perp} . In this condition, the peak at higher field shifts to higher field as L_{\perp} is reduced and sharply diverge at the critical length of L^* .

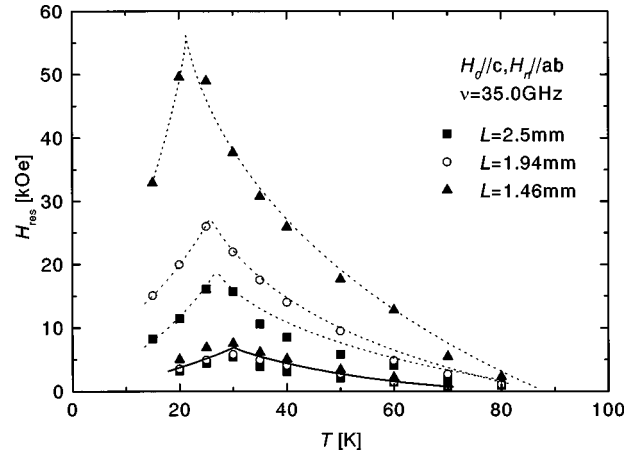


FIG. 5. Temperature dependence of the transverse Josephson plasma resonance field for three different dimensions of the ab plane, 2.5, 1.94, and 1.46 mm. Dotted and solid lines are a guide to the eye.

The sample dimension L_{\perp} is actually changed from 2.50 to 0.737 mm. The largest size is limited by the cavity size. In contrast, the lower resonance does not move despite changing the sample size. We note that the resonance absorption at the lower field remains at the same field, similar to the one for $E_{rf} \parallel c$, although the intensity decreases as the size is reduced. We have checked the influence of the L_{\parallel} on the reso-

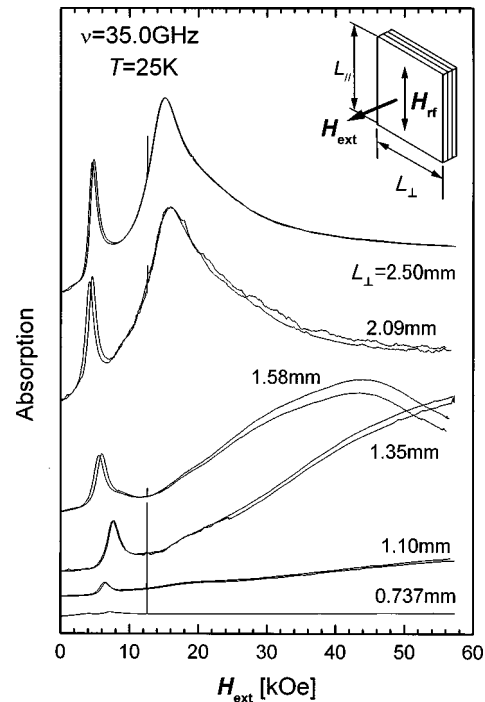


FIG. 6. The absorption lines observed in sample A at 25 K at a various sample dimensions of the ab plane. The detailed sample geometry as well as the configuration between the microwave H_{rf} and external field H_{ext} is shown in the inset. The sample size is reduced along one direction step by step, and the length along the other direction is fixed at 2.4 mm. The broad resonance at a higher field shifts to higher fields as L decreases, while the sharp resonance at the lower field does not move. The absorption intensity decreases as L is decreased.

nance field \mathbf{H}_{res} for the case in $\mathbf{H}_{\text{rf}} \parallel ab$. It is experimentally confirmed that the resonance line did not shift at all.

As seen in Figs. 4 and 6, the characteristic feature in the case of $\mathbf{H}_{\text{rf}} \parallel ab$ is the line shape. The lower field line is sharp and has more or less a symmetric line shape, in strong contrast to the higher field line, which exhibits broad and rather asymmetric line shapes with a strong tail at the higher field side. When the sample size is reduced to the critical dimension L^* , the resonance line shifts sharply to the higher field side and becomes extremely broad, then disappears at L^* . Although the higher field resonance line is influenced by the dimension, the lower field line does not shift at all. The smallest sample dimension in this case was $L=0.737$ mm, limited by the detection limit of the resonance intensity.

IV. DISCUSSION

In this section, we will discuss the nature of the resonance which is observed under two different configurations, $\mathbf{E}_{\text{rf}} \parallel c$ and $\mathbf{H}_{\text{rf}} \parallel ab$. We take the x and y axes in the ab plane and the z axis along the c axis of the samples in the following discussion.

A. Plasma excitation with a perpendicular oscillating electric field: longitudinal plasma

As described in Fig. 1, the sample is placed at the center of the cross section of the cavity at a distance $\lambda_g/4$ above the bottom of the cavity. In this case, the oscillating electric field \mathbf{E}_{rf} acts uniformly on the sample. (The inhomogeneity of the \mathbf{E}_{rf} in the sample with $1 \text{ mm} \times 1 \text{ mm}$ size is estimated to be less than 5% over the sample.) Moreover, it is advantageous that, in this cavity mode, the electric vector \mathbf{E}_{rf} can be separated from the magnetic vector \mathbf{H}_{rf} without complication. This condition cannot be met by other cavity modes such as the cylindrical ones. If the external electric field \mathbf{E}_{rf} is uniform in the ab plane, we can assume that the phase difference between the layers is also uniform in the direction parallel to the layers. As is well known, the gauge-invariant phase difference between $l+1$ th and l th layers is defined by

$$\varphi_{l+1,l}(t) = \varphi_{l+1}(t) - \varphi_l(t) - \frac{2\pi}{\phi_0} \int_{z_l}^{z_{l+1}} dz A_z(z, t), \quad (1)$$

where $\phi_0 = hc/2e$, $\varphi_l(t)$ is the phase of the order parameter on the l th superconducting layer and $A_z(z, t)$ is the z component of the vector potential. The oscillating electric field \mathbf{E}_{rf} induces the current through the $l+1$ th and l th layers, which consists of Josephson current $j_c \sin \varphi_{l+1,l}(t)$, quasiparticle current $\sigma_{\text{qp}} E_{l+1,l}(t)$, and displacement current $(\epsilon/4\pi) \times (\partial/\partial t) E_{l+1,l}(t)$, and can be expressed as

$$J = j_c \sin \varphi_{l+1,l}(t) + \sigma_{\text{qp}} E_{l+1,l}(t) + \frac{\epsilon}{4\pi} \frac{\partial}{\partial t} E_{l+1,l}(t), \quad (2)$$

where j_c is the Josephson critical current density, σ_{qp} is the conductivity for the quasiparticle current, and ϵ is the high-frequency dielectric constant of the insulating block layers, respectively. If the charging effect is taken into account, the Josephson relation of the phase difference $\varphi_{l+1,l}(t)$ and the voltage difference $V_{l+1,l}(t)$ between the layers is shown as²²

$$\frac{\hbar}{2e} \frac{\partial}{\partial t} \varphi_{l+1,l}(t) = \frac{\epsilon \mu^2}{sD} \left[-V_{l,l-1}(t) + \left(2 + \frac{sD}{\epsilon \mu^2} \right) \times V_{l+1,l}(t) - V_{l+2,l+1}(t) \right], \quad (3)$$

where s and D are the thickness of the CuO_2 and the block layers, and μ is the screening length of the superconducting charge, which is much shorter than the London penetration depth λ_c . This equation (3) is the modified Josephson relation for the case of thin electrodes and can be reduced to the conventional Josephson relation when $\epsilon \mu^2/sD \rightarrow 0$. Combining Eqs. (2) and (3), we have the equation for the gauge-invariant phase difference:

$$\begin{aligned} \frac{\epsilon}{c^2} \frac{\partial^2}{\partial t^2} \varphi_{l+1,l}(t) &= \frac{\alpha}{\lambda_c^2} [\sin \varphi_{l+2,l+1}(t) - (2 + \alpha^{-1}) \\ &\times \sin \varphi_{l+1,l}(t) + \sin \varphi_{l,l-1}(t) \\ &+ \beta \{ V_{l+2,l+1}(t) - (2 + \alpha^{-1}) V_{l+1,l}(t) \\ &+ V_{l,l-1}(t) \}] + \frac{J}{\lambda_c^2 j_c}, \end{aligned} \quad (4)$$

where $\alpha = \epsilon \mu^2/sD$, $\beta = e\sigma/\pi D j_c$, and $\lambda_c = \sqrt{c\phi_0/8\pi^2 D j_c}$ is the penetration length along the c axis. The solution of Eq. (4) for $J=0$ and $\sigma_{\text{qp}}=0$ gives the dispersion relation of the longitudinal Josephson plasma as

$$\begin{aligned} \omega_L(k_z) &= \omega_p \sqrt{1 + \frac{2\epsilon \mu^2}{D^2} [1 - \cos(k_z D)]}, \\ &\approx \omega_p \sqrt{1 + \epsilon \mu^2 k_z^2}, \end{aligned} \quad (5)$$

with $\omega_p = c/\sqrt{\epsilon} \lambda_c$. Since $\epsilon \sim 10$ and $\mu \sim 10 \text{ \AA}$, this dispersion relation is almost independent of k_z in the microwave frequency region ($k_z \sim 1 \text{ cm}^{-1}$). Although the excited plasma is represented by the superposition of the standing waves with wave number $k_{2n+1} = (2n+1)\pi/d$, with n and d being the integer and thickness of the sample, the longitudinal plasma resonance has a sharp and little asymmetry of the line shape because of the dispersionless character of the longitudinal plasma expressed by Eq. (5). Similar results have been reported earlier by Bulaevskii *et al.*³⁵ for arbitrary k , although they do not take into account the charge screening effect.

In this experiment, d is fixed for all L , and ω_L is not sensitive to k_z because of the flat dispersion. Therefore, ω_L changes little unless d varies drastically. Experimental results¹³ indicate that the plasma frequency ω_p depends on H_{ext} as $\omega_p \propto H_{\text{ext}}^{-1/2}$, which enables us to rewrite ω_L/ω_p as $(H_{\text{ext}}/H_0)^{1/2}$, where $H_0 = \Gamma^2/\omega_L^2$ is the resonance field. Using this equation, it is found that the resonance field is also independent of L . The observed resonance field is indeed independent of L within the experimental error. This agrees with the theoretical predictions discussed above.

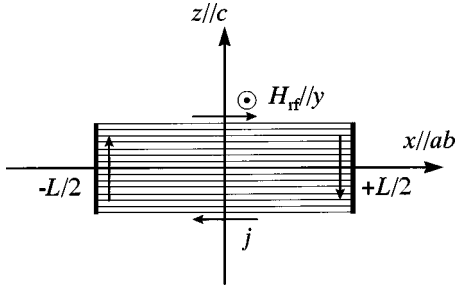


FIG. 7. Schematic diagram of the crystal with microwave component $H_{rf}\parallel y$ for the transverse plasma excitation. The solid arrows indicate the hypothetical external current (j) induced by H_{rf} . The current parallel to the c axis penetrates much deeper than the one parallel to the ab plane because λ_c/λ_{ab} is as large as 1000 in $\text{Bi}_2\text{Sr}_2\text{CaCu}_2\text{O}_{8+\delta}$. This current along the c axis drives the oscillating electric field of E_{rf} , which excites the transverse Josephson plasma.

B. Plasma excitation with a parallel oscillating magnetic field: transverse plasma

Let us consider a layered system whose dimension is L along the x axis and infinity along y and z axes as displayed in Fig. 7. When H_{rf} is applied parallel to the y axis with uniform intensity within the ab plane, the screening current j is induced. As a result, the electric field E is formed in accordance with the Maxwell's equations and the London equation as follows:

$$\frac{4\pi}{c}j = -\frac{1}{\lambda_c^2}A, \quad (6)$$

$$\nabla \times \mathbf{B} = \frac{4\pi}{c}(j + \sigma_{qp}E) + \frac{\epsilon}{c} \frac{\partial}{\partial t}E, \quad (7)$$

$$\nabla \times E = -\frac{1}{c} \frac{\partial}{\partial t}B, \quad (8)$$

where $j = (0, 0, j_z)$, $A = (0, 0, A_z)$, $B = (0, B_y, 0)$, and $E = (0, 0, E_z)$. The normal mode of the electromagnetic wave inside the superconductor can be obtained by setting $B_y \propto \exp[ikx - i\omega t]$ into the Maxwell's equations (7) and (8). As a result, the following condition has to be satisfied:

$$k^2 + \frac{1}{\lambda_c^2} - \frac{4\pi}{c^2}i\omega\sigma_{qp} - \frac{\epsilon}{c^2}\omega^2 = 0, \quad (9)$$

where k is defined as $k = k' + ik'' = (\omega/c)\sqrt{\epsilon(\omega)}$. Since B_y must satisfy the boundary condition at $x = \pm L/2$ as $B(\pm L/2) = H_{rf}$, B_y can be obtained as

$$B_y = H_{rf}e^{-i\omega t} \left[\frac{e^{ikx} + e^{-ikx}}{e^{ikL/2} + e^{-ikL/2}} \right]. \quad (10)$$

Therefore, the electric field E_z can be displayed as

$$E_z = -i\frac{\omega}{c} \int^x B_y dx = -\frac{\omega H_{rf}}{ck} e^{-i\omega t} \left[\frac{e^{ikx} - e^{-ikx}}{e^{ikL/2} + e^{-ikL/2}} \right]. \quad (11)$$

The power absorption $\varphi = \int_{-L/2}^{L/2} dx \langle \text{Re}j \cdot \text{Re}E \rangle_t$ can be rewritten as

$$\varphi = \frac{1}{2} \sigma_{qp} \int_{-L/2}^{L/2} dx |E_z|^2 = \frac{L}{2} H_{rf}^2 \frac{\sigma_{qp}}{\epsilon(\omega)} \times \left(\frac{\sinh k''L/k'L - \sinh k'L/k'L}{\cosh k''L + \cosh k'L} \right), \quad (12)$$

where $\epsilon(\omega) = \epsilon(1 - \omega_p^2/\omega^2) + 4\pi i\sigma_{qp}/\omega$. Since the resonance peaks originate from the pole of Eq. (12), this condition yields either $\epsilon(\omega) = \epsilon(1 - \omega_p^2/\omega^2) = 0$ or $1 + \cos((\omega/c)\sqrt{\epsilon(\omega)}L) = 0$. The former equation leads the fundamental resonance at $\omega = \omega_p$, while the latter equation gives the multiple resonance at the frequencies given as

$$\frac{\omega_n^2}{\omega_p^2} = \frac{1}{1 - [(2n-1)\pi/\{\sqrt{\epsilon}L/(c/\omega)\}]^2}. \quad (13)$$

As mentioned before, we can rewrite ω^2/ω_p^2 for H/H_0 , thus the resonance field is determined by Eq. (13),

$$\frac{H_n}{H_0} = \frac{1}{1 - [(2n-1)\pi/\{\sqrt{\epsilon}L/(c/\omega)\}]^2}, \quad (14)$$

where H_0 denotes the resonance field of the large L limit. This implies that the multiple-resonance lines may be observed, depending on the sample size L . For instance, double resonance lines are observable with condition of $4.05 \text{ mm} \leq L \leq 6.75 \text{ mm}$ for $\epsilon = 10$ and $\omega/2\pi = 35 \text{ GHz}$, whereas a single resonance is expected in $1.35 \text{ mm} \leq L \leq 4.05 \text{ mm}$. It is noted that there is only a fundamental mode when the sample size is smaller than 1.35 mm.

Figure 8 shows the experimental results of the resonance field as a function of L . The resonance lines show the sharp divergent behavior as the sample size is reduced. The solid lines are the fitted curves using Eq. (14) with a single parameter ϵ . As seen in Fig. 8 the agreement between the experimental results and the fitted curve is excellent. From this analysis the value of $\epsilon = 8.47$ is deduced.

V. SUMMARY

We have measured the Josephson plasma resonance as a function of the sample size L , and characterized the longitudinal and the transverse plasma modes. It is of importance to stress here that the two plasma modes were experimentally separated out and were identified independently.

The longitudinal plasma is excited by a perpendicular oscillating electric field ($E_{rf}\parallel c$), exerted uniformly in the ab plane. Since the resonance field, which is equivalent to the Josephson plasma frequency, is independent of the dimension in the ab plane in this case, the longitudinal plasma, which propagates with the wave vector k perpendicular to the layers, is actually independent of $|k|$.

In contrast, by applying the parallel oscillating magnetic field ($H_{rf}\parallel ab$), the transverse plasma can be generated, which propagates parallel to the ab plane. Therefore, the Josephson plasma resonance observed in this configuration

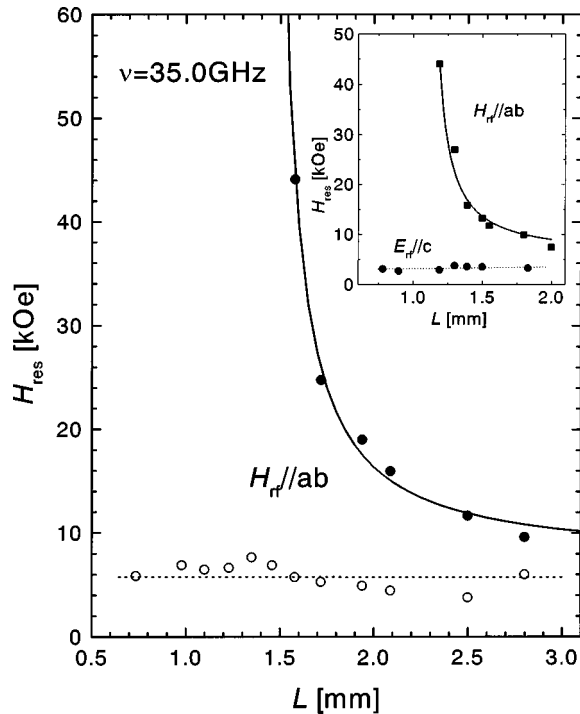


FIG. 8. The resonance field diagram for sample A as a function of the sample size L at 35 GHz and 25 K. The solid symbols indicate the transverse plasma resonance, which shows divergent character in the case of $H_{r\parallel}||ab$, and solid lines indicate the fitted results by Eq. (18). The open symbols represent the sharp resonance field which appears at the lower field. The horizontal dotted line is a guide to the eye. The inset displays the same diagram for sample B in which the size dependence of the resonance in $E_{r\parallel}||c$ was also measured.

strongly reflects the dispersion relation. This results in the appearance of the strong ab -plane size dependence. The shift of the resonance field by reduction of L is quantitatively explained by Eq. (14) with a single parameter ϵ , and is in good agreement with the picture of the layered superconducting system with finite size of the plane.^{24,25} The result of the fitting gives the value $\epsilon = 8.47$. This good agreement ensures that the theoretical model used here is appropriate to describe the Josephson plasma phenomena. This sharply contradicts the approach given by Bulaevskii *et al.*,^{15–17,35} who do not take into account the charge screening effect in their treatment, although the final result is almost identical. This charge screening effect is the most essential difference in the layered system such as $\text{Bi}_2\text{Sr}_2\text{CaCu}_2\text{O}_{8+\delta}$ in comparison with the conventional Josephson junctions.

According to the concept of the spontaneously broken symmetry, the symmetry of the phase degree of freedom of

the gauge field is broken in the superconducting transition.^{26–29} The longitudinal plasma mode is the collective excitation mode, also called the phason mode or the Nambu-Goldstone mode.^{30,31} However the transverse plasma mode is not the Nambu-Goldstone mode in a superconductor.

In a conventional superconductor, the plasma modes (both longitudinal and transverse mode) have an energy gap, which is of the order of eV, far beyond the superconducting energy gap of a few meV. This energy gap was predicted by Anderson,²⁶ who took into account the long-range Coulomb interaction effect in the theory of superconductivity. The energy level is identical to the plasma energy in the normal state, which lies at such high energies that the excitation mode cannot be distinguished from the quasiparticle excitations with the strong Landau damping. Therefore, there has been no experimental confirmation of the plasma mode in a superconductor, especially the longitudinal plasma mode (Nambu-Goldstone mode).

The Josephson plasma mode is nothing but the superconducting plasma mode associated with the Josephson Cooper pair tunneling through insulating layers, and has been proved to exist in the present high- T_c superconductor $\text{Bi}_2\text{Sr}_2\text{CaCu}_2\text{O}_{8+\delta}$.^{17,22,30} As explained in Sec. III, we were able to separate the two Josephson plasma modes experimentally. This enables us to identify the longitudinal Josephson plasma mode separately from the transverse one. This was experimentally carried out by measuring the sample size dependence of the resonance, which is derived from the difference in the dispersion relations of the two modes. The experimental result agrees very well with the theoretical prediction as described in Sec. IV. Therefore, it is concluded that we have experimentally confirmed the existence of the Nambu-Goldstone mode in a superconductor, which has a finite gap as described by the Anderson-Higgs mechanism.^{29,32,33} We also note that although the Carlson-Goldman mode³⁶ in a conventional Josephson junction was shown to be the Nambu-Goldstone mode, the excitation is only possible with strong coupling between Cooper pairs and quasiparticles. Therefore, this excitation may be only observable in the very vicinity of T_c .

ACKNOWLEDGMENTS

The authors would like to express their gratitude to Professor M. Tachiki and Professor T. Koyama for their theoretical suggestions. This work has been supported by CREST (Core Research for Evolutional Science and Technology) of the Japan Science and Technology Corporation (JST) and is also supported in part by the Research Projects (category A), The University of Tsukuba.

¹T. W. Noh, S. G. Kaplan, and A. J. Sievers, Phys. Rev. B **41**, 307 (1990).

²K. Tamasaku, Y. Nakamura, and S. Uchida, Phys. Rev. Lett. **69**, 1455 (1992).

³M. Tachiki, T. Koyama, and S. Takahashi, Phys. Rev. B **50**, 7065 (1994).

⁴A. A. Abrikosov, *Fundamentals of Theory of Metals* (North-

Holland, Amsterdam, 1988), Chap. 16.

⁵R. Kleiner and P. Müller, Phys. Rev. B **49**, 1327 (1994).

⁶R. Kleiner, F. Steinmeyer, G. Kunkel, and P. Müller, Phys. Rev. Lett. **68**, 2394 (1992).

⁷G. Oya, N. Aoyama, A. Irie, S. Kishida, and H. Takuhata, Jpn. J. Appl. Phys., Part 2 **31**, L829 (1992).

⁸K. Kadowaki and T. Mochiku, Physica B **194-196**, 2239 (1994).

- ⁹H. A. Fertig and S. Das Sarma, Phys. Rev. B **44**, 4480 (1991).
- ¹⁰T. M. Mishonov, Phys. Rev. B **44**, 12 033 (1991).
- ¹¹T. Hasegawa, M. Naitoh, and K. Kitazawa, Jpn. J. Appl. Phys., Part 2 **30**, L276 (1991).
- ¹²C. Renner, Ph.D. thesis, University Geneva, 1995.
- ¹³Ophelia K. C. Tsui, N. P. Ong, Y. Matsuda, Y. F. Yan, and J. B. Peterson, Phys. Rev. Lett. **73**, 724 (1994).
- ¹⁴Y. Matsuda, M. B. Gaifullin, K. Kumagai, K. Kadowaki, and T. Mochiku, Phys. Rev. Lett. **75**, 4512 (1995).
- ¹⁵L. N. Bulaevskii, M. P. Maley, and M. Tachiki, Phys. Rev. Lett. **74**, 801 (1995).
- ¹⁶L. N. Bulaevskii, V. L. Pokrovsky, and M. P. Maley, Phys. Rev. Lett. **76**, 1719 (1996).
- ¹⁷L. N. Bulaevskii, D. Dominguez, M. P. Maley, A. R. Bishop, Ophelia K. C. Tsui, and N. P. Ong, Phys. Rev. B **54**, 7521 (1996).
- ¹⁸A. E. Koshelev, Phys. Rev. Lett. **77**, 3901 (1996).
- ¹⁹Ophelia K. C. Tsui, N. P. Ong, and J. B. Peterson, Phys. Rev. Lett. **76**, 819 (1996).
- ²⁰S. Sakamoto, A. Maeda, T. Hanaguri, Y. Kotaka, J. Shimoyama, K. Kishio, Y. Matsushita, M. Hasegawa, H. Takei, H. Ikeda, and R. Yoshizaki, Phys. Rev. B **53**, R14 749 (1996).
- ²¹T. Shibauchi, M. Sato, A. Mashio, T. Tamegai, H. Mori, S. Tajima, and S. Tanaka, Phys. Rev. B **55**, 11 977 (1997).
- ²²M. Tachiki, T. Koyama, and S. Takahashi, in *Coherence in Superconductors*, Proceedings of the International Workshop on Coherence in High T_c Superconductors, May 1–3, 1995, held in Herzlia, Israel, edited by G. Deutscher and A. Revcolevschi (World Scientific, Singapore, 1996).
- ²³K. Kadowaki, M. B. Gaifullin, Y. Matsuda, K. Kumagai, S. Takahashi, and M. Tachiki, Czech. J. Phys. **46**, Suppl. S3, 1625 (1996).
- ²⁴S. Takahashi, M. Tachiki, I. Kakeya, K. Kindo, T. Mochiku, and K. Kadowaki, Physica C **293**, 64 (1997).
- ²⁵I. Kakeya, K. Kindo, K. Kadowaki, and T. Mochiku, Physica C **282-287**, 1599 (1997).
- ²⁶P. W. Anderson, Phys. Rev. **110**, 827 (1958).
- ²⁷G. Ryckayzen, Phys. Rev. **111**, 817 (1958).
- ²⁸Y. Nambu, Phys. Rev. **117**, 648 (1960).
- ²⁹J. Goldstone, A. Salam, and S. Weinberg, Phys. Rev. **127**, 965 (1962).
- ³⁰K. Kadowaki, I. Kakeya, M. B. Gaifullin, T. Mochiku, S. Takahashi, T. Koyama, and M. Tachiki, Phys. Rev. B **56**, 5617 (1997).
- ³¹K. Kadowaki, I. Kakeya, and K. Kindo (unpublished).
- ³²P. W. Anderson, Phys. Rev. **112**, 1900 (1958).
- ³³P. Higgs, Phys. Rev. **145**, 1156 (1966).
- ³⁴T. W. B. Kibble, Phys. Rev. **155**, 1554 (1967).
- ³⁵L. N. Bulaevskii, M. Zamora, D. Baeriswyl, H. Beck, and John R. Clem, Phys. Rev. B **50**, 12 831 (1994).
- ³⁶R. V. Carlson and A. M. Goldman, Phys. Rev. Lett. **34**, 11 (1975).